

Supporting Information for:

Anisotropy Effects on The Kinetics of Colloidal Crystallization and Melting: Comparison of Spheres and Ellipsoids

Peng-Kai Kao^a, Bryan J. VanSaders^b, Michael D. Durkin^a, Sharon C. Glotzer^{a,b} and Michael J. Solomon^a

^aDepartment of Chemical Engineering, University of Michigan, Ann Arbor, Michigan

^bDepartment of Materials Science & Engineering, University of Michigan, Ann Arbor, Michigan

Corresponding Author

Prof. Michael J. Solomon

Address: North Campus Research Complex, Building 10 – A151, 2800 Plymouth Road, Ann Arbor, MI 48109

Phone: 734 -764-3119

Email: mjsolo@umich.edu

1. Molecular Dynamics Methods

Simulations of colloid assembly and disassembly were carried out with HOOMD-Blue^{1,2}, using Langevin dynamics integration. The experimental forces present on colloidal particles arise from several sources and were represented using different simulated analogs. Figure 4 (a) schematically illustrates the particle interaction model used. Simulation units can be converted to physical units by choosing a set of self-consistent base units. Thermal energy can be converted to temperature by the expression $T_{phys} = E k T_{sim} / k_b$, where E is the energy base unit and k_b is Boltzmann's constant in units matched to E . By choosing E to be the energy required to lift the polystyrene ellipsoids used in this study (immersed in water) by two times their minor axis, the simulation thermal energy of 0.1 corresponds to 300K. Other energies reported here are given in terms of this thermal energy. In our simulations, the mass unit is taken to be the mass of one polystyrene sphere of diameter 4 μ m. The distance unit is the sphere diameter. With these units and the energy unit, the conversion factor for time is $\tau = \sqrt{m D^2 / \epsilon}$, where m , D , and ϵ are the mass, distance, and energy units respectively.

Particle-particle interactions are modeled using a Gay-Berne ellipsoidal potential³ to represent hard core anisotropic repulsion and mild direction-independent attraction. The value of ϵ in the Gay-Berne potential is chosen as $2.0 k T$. For particles in quasi-2D, this is insufficient to induce condensation into a dense fluid. The major and minor axes of the prolate ellipsoid represented by this potential are chosen so that the minimum-energy isosurface encloses the same volume for spheres (minor axis equal to major) and ellipsoids (axis ratio of 2). The Gay-Berne potential was truncated at a distance of 4 times the major axis of the particles being simulated.

Anisotropic attractions and repulsions between particles are the result of electrostatic forces as particles are polarized in the AC electric field device used for self-assembly. This induced polarization is represented discretely, following Crassous *et al.*⁴ Rigid bodies² were used to enforce the relative orientation and position of two charge-representing particles (positive and negative) placed on the ellipsoid major axis with respect to the ellipsoid center. The separation of these charge-representing particles was chosen to be a function of aspect ratio (α), linearly decreasing from 1.75 times the particle major axis length at $\alpha = 1.0$ and 1.6 times the particle major axis length

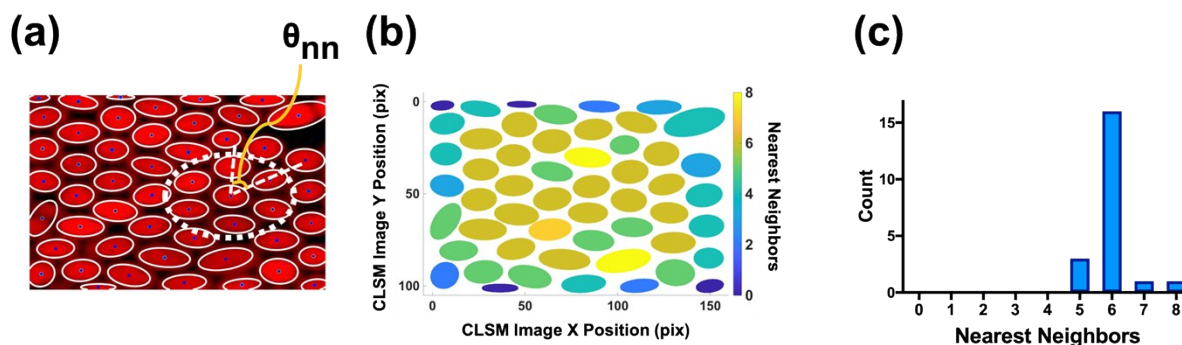
at $\alpha = 2.0$. These values are chosen to reproduce the experimentally observed crystal structure of 2D assemblies at $\alpha = 1.0$ and $\alpha = 2.0$. The charge-representing particles have their interaction strength scaled to a common value for the closest distance of approach at the Gay-Berne minimum-energy isosurface. For spheres, this distance is parallel to the applied field direction. As α is increased, the closest distance from a point on the major axis to the ellipsoid edge is no longer parallel to the field direction. By choosing to scale charged interactions in this way, the simulation model matches the sphere-sphere and ellipsoid-ellipsoid electrostatic bond strength. Charge based particle-particle bonds are compared at a common strength for spheres and ellipsoids. This focuses the model on the effect of geometric changes of the particle's shape. The value of all charge-mediated bonds was scaled to $6kT$ at the surface of the ellipsoidal repulsion. The electrostatic interactions were truncated at a range equal to twice the diameter of the simulated spheres.

In experiment, ellipsoids are observed to align with the electric field direction, as reported in the main text. The alignment force is represented in simulation by a constant force applied (in opposite directions) to each charge-representing particle. To determine the strength of these alignment forces, a maximum angle is chosen. The forces are then scaled so that the integrated work of turning a particle from alignment with the field to the chosen angle while under these forces is equal to kT . In this parameterization scheme, the maximum deviations of particle alignment from the force direction during a thermalized simulation are approximately equal to the chosen maximum angle. For all simulated systems shown here, the maximum angle was chosen to be 60° .

Sedimentation is represented in simulation by the application of a constant downward force and a repulsive wall in the xy-plane. For all systems shown here this force was chosen as $F = 20kT/D$, where D is the diameter of an $\alpha = 1.0$ particle. This force is applied to the particle centers. Ellipsoidal particles are prevented from rotating out of plane when the alignment field is turned off by the repulsive effect of the wall. The wall interacts with particle centers and charge-representing particles via a Weeks-Chandler-Andersen⁵ repulsive potential. Any rotation of particles out of plane forces the body center to a higher z-position, thereby incurring an energy penalty. All particle simulations shown here are systems with 10,000 colloid particles. All boundaries are periodic.

Model parameter fitting to recapitulate the observed experimental crystal structure, which was then the basis for the characterization of kinetics, was most sensitive to the position of the charge-representing particles within the repulsive core. For ellipsoidal particles, different separations of the charged particles along the major axis can produce the crystal structure experimentally observed for spheres or that observed for $\alpha = 2$ ellipoids. For spheres, the preferred motif of charge-mediated interactions is to form chains. Inter-chain attraction due to charge forces alone was too weak to result in long range 2D crystals. The attractive component of the Gay-Berne potential was needed to provide a weak direction-independent attraction in order for spheres to fully order. Given the unknowns present in the electrodynamics of the fluid and particle polarizations, applying an isotropic attraction in this manner was deemed an appropriate, parsimonious approximation. Changes to the angular freedom of particles under ‘field-on’ conditions were not found to have strong consequences for phase behavior of the model, but instead introduced additional spread into the peaks present in the Fourier domain representation of the crystals. The magnitude of the downward force (representing the effect of particle settling) needed to be sufficiently large to prevent the formation of 3D cluster assemblies but was otherwise unimportant.

2. Structural Characterization

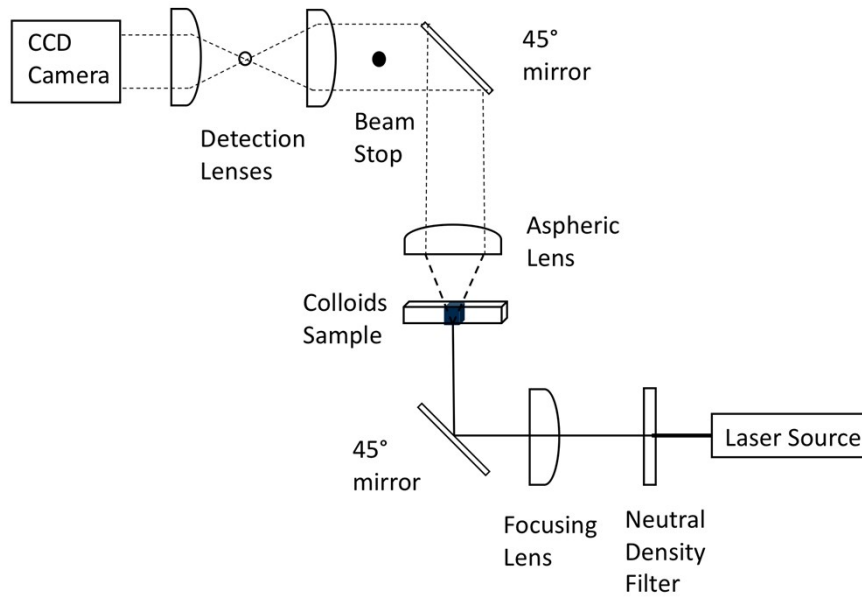


S1. (a) The white dotted region illustrates the elliptic coordination shell for determining the positional order parameters, including the nearest neighbors and the nearest neighbor angles of a self-assembled structure. (b) The map of local nearest neighbors of the close-packed assembly as shown in S1-(a). (c) The counts of nearest neighbors of the close-packed assembly as shown in S1-(a). Particles at the edge are excluded in the counting.

In this study, we determine the number of nearest neighbors of a colloid as those within a set radius of that colloid's surface. We set this radius of the elliptic coordination shell to be 2.1 times the second peak of $g(r)$ of the close-packed colloidal ellipsoids array, as shown in S1 (a). The overall positional order of the assembly environment of S1 (a) is shown in S1 (b). Particles at the periphery of the microscopic image are not considered because all their neighbors cannot be identified due to boundary effects. S1 (c) shows that for the close-packed assembly in S1 (a), 76% of the ellipsoidal particles have six nearest neighbors. The average number of nearest neighbors of this assembly is 6.0 ± 0.6 .

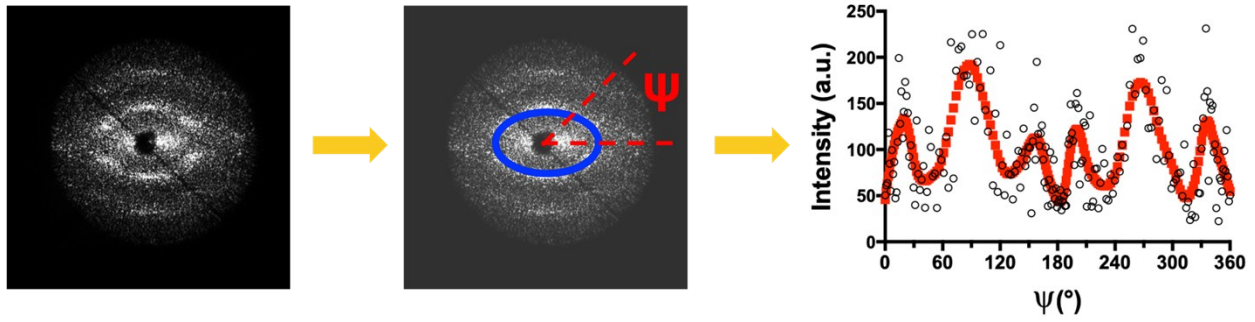
We computed nearest neighbor angles, θ_{nn} , from CLSM images as another local order parameter to quantify short-range positional order of colloidal assemblies. θ_{nn} are the angles between each two adjacent vectors within the elliptic coordination shell. For example, for each spherical particle in a hexagonally close-packed assembly, there are six nearest neighbor angles, each with the value of 60° .

3. Small-angle Light Scattering Apparatus and Characterization



S2. Schematic of the small-angle light scattering apparatus.

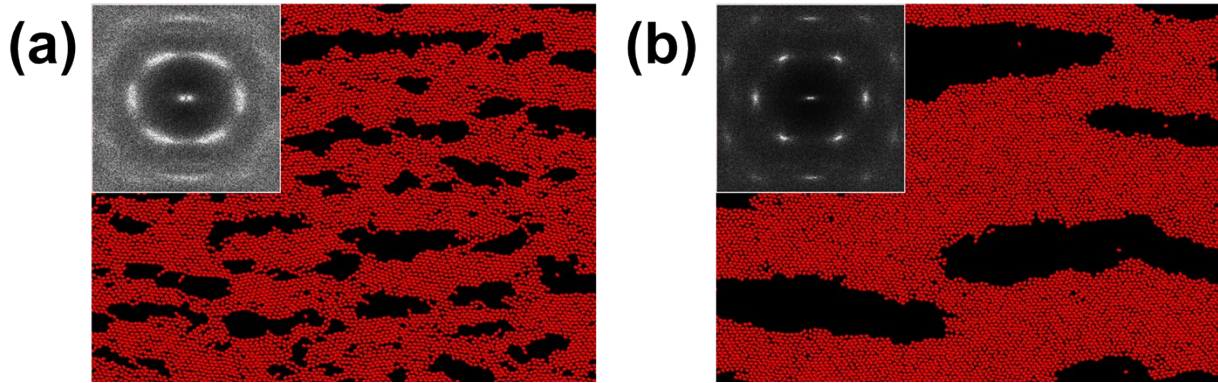
The small-angle light scattering (SALS) device collects real-time light diffraction measurements over the angular range of 2° - 13° . The performance of the device, assessed by comparison to calculations by Mie scattering theory, is good to within 12.5% from 2° to 12° .



S3. Analysis of the small-angle light scattering (SALS) data. In the first order scattering peaks (the blue elliptical ring), ψ is defined as the angle between the semi-major axis of the elliptical ring and the line connecting a peripheral point to the centroid of the elliptical ring. The intensity of light scattering responses varies at each ψ within the first order scattering responses.

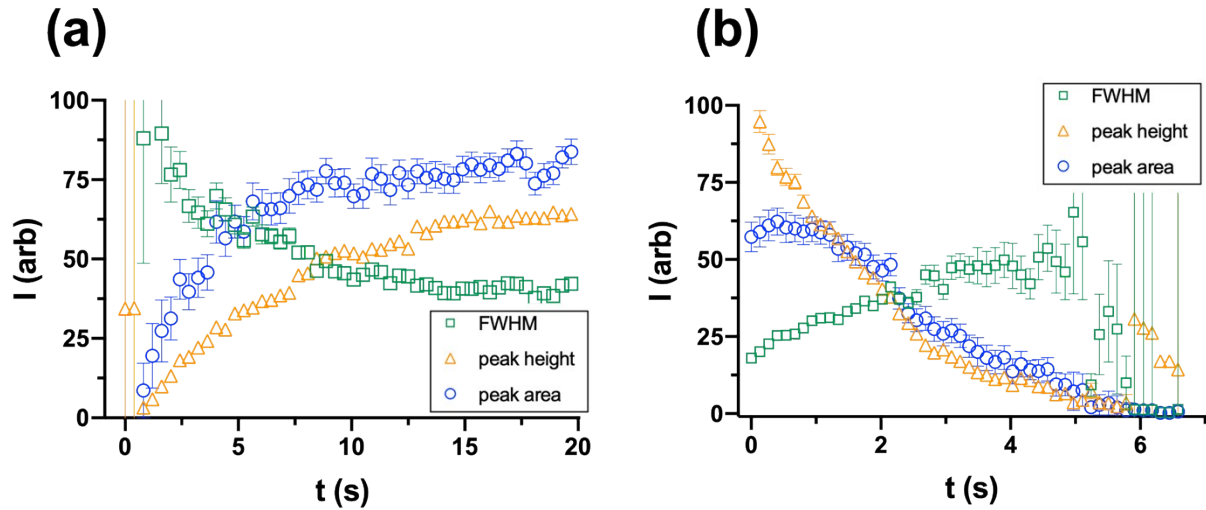
The blue ring shown in S3 has a finite width of 31 pixels due to the average width of the primary scattering patterns being 31 ± 2 pixels.

4. Evolution of Grain Microstructure by Molecular Dynamics



S4. The evolution of simulated grain microstructure. (a) System snapshot and Fourier domain pattern for ellipsoids with an axis ratio of 1.4 after 20 seconds of simulated time with the field on. (b) The same system after 11 minutes of simulated field-assisted assembly. Differences in the system's Fourier domain pattern and void structure are due to grain boundary annealing.

5. Comparison of Different SALS Measures



S5. Comparison of different measures of a simulated SALS peak during (a) assembly and (b) melting for spheres. The intensities of curves have been scaled to allow comparison across the panels of the figure. The time scale of all curves is equivalent; however, the curve shape of peak area is most favorable for fitting as a useful convolution of the two other states, namely a low peak area state and high peak area state. In this study peak area is used, but equivalent conclusions can be drawn from any of these measures of the diffraction peaks.

References

- 1 J. A. Anderson, C. D. Lorenz and A. Travesset, *J. Comput. Phys.*, 2008, **227**, 5342–5359.
- 2 T. D. Nguyen, C. L. Phillips, J. A. Anderson and S. C. Glotzer, *Comput. Phys. Commun.*, 2011, **182**, 2307–2313.
- 3 J. G. Gay and B. J. Berne, *J. Chem. Phys.*, 1981, **74**, 3316–3319.
- 4 J. J. Crassous, A. M. Mihut, E. Wernersson, P. Pflaiderer, J. Vermant, P. Linse and P. Schurtenberger, *Nat. Commun.*, 2014, **5**, 5516.
- 5 J. D. Weeks, D. Chandler and H. C. Andersen, *J. Chem. Phys.*, 1971, **54**, 5237–5247.